Interactions of mineral dust particles and clouds: Effects on precipitation and cloud optical properties

Yan Yin,[1] Sabine Wurzler,[2] Zev Levin,[3] and Tamir G. Reisin[4]

Received 29 November 2001; revised 22 April 2002; accepted 12 June 2002; published 14 December 2002.

[1] Numerical simulations were performed to investigate the effect of cloud-processed mineral dust particles on the subsequent development of cloud and precipitation and possible effects on cloud optical properties. A two-dimensional (2-D) nonhydrostatic cloud model with detailed microphysics was used. The initial aerosol spectra used in the 2-D model consisted of both background cloud condensation nuclei and mineral dust particles. These were taken from the results of three successive runs of a parcel model that simulates the interaction of dust and sulfate particles with cloud drops and trace gases and then evaporates the cloud drops. The results show that insoluble mineral dust particles become effective cloud condensation nuclei (CCN) after passing through a convective cloud. Their effectiveness as CCN increases because of a layer of sulfate that is formed on their surface as they are first captured by growing drops or ice crystals and then released as these hydrometeors evaporate. Upon entering subsequent clouds, these particles increase the concentration of the activated drops and widen the drop size distribution. The present work shows that in continental clouds the effect of cloud-processed dust particles is to accelerate the formation of precipitation particles, although the amount of precipitation depends on the concentration of the large and giant CCN. In maritime clouds the addition of cloud-processed aerosol and mineral dust particles has a minimal effect on precipitation because the cloud starts with many large particles already. The addition of more CCN to either maritime or continental clouds increases their optical depth, even for those cases in which the precipitation amount is increased. *INDEX TERMS:* 0320 Atmospheric Composition and Structure: Cloud physics and chemistry; 0305 Atmospheric Composition and Structure: Aerosols and particles (0345, 4801); 3337 Meteorology and Atmospheric Dynamics: Numerical modeling and data assimilation; 3354 Meteorology and Atmospheric Dynamics: Precipitation (1854); *KEYWORDS:* cloud processing, dust, cloud modeling, cloud optical properties

Citation: Yin, Y., S. Wurzler, Z. Levin, and T. G. Reisin, Interactions of mineral dust particles and clouds: Effects on precipitation and cloud optical properties, *J. Geophys. Res.*, *107*(D23), 4724, doi:10.1029/2001JD001544, 2002.

1. Introduction

[2] Aerosol particles have a major influence on the energy budget of the atmosphere. They not only have a direct influence on the radiation balance by scattering and absorbing solar and terrestrial radiation, but also an indirect effect on the energy budget by modifying the microphysics of clouds [*Twomey*, 1977; *Hansen et al.*, 1998]. Furthermore, they have a major impact on the efficiency of growth of hydrometeors (drops, graupel particles and ice crystals) and through it on the amount and location of the release/removal of latent heat (by condensation/evaporation and freezing/melting processes). At the same time, clouds themselves modify the aerosol particle concentrations and composition due to coagulation, sedimentation, liquid phase chemical reactions and evaporation of drops [e.g., *Wurzler et al.*, 2000]. In turn, by interacting with other clouds, these modified aerosol particles can influence the microphysical characteristics and the formation of precipitation in subsequent clouds.

[3] Mineral dust is one of the main natural sources of atmospheric aerosol particles and is observed even in the most remote regions of the world. Measurements of aerosol particle composition in the Mediterranean region reveal that sulfate is found in most aerosol particles. Among these are mineral dust particles that are coated with sulfate as well as with other soluble substances [e.g., *Fonner and Ganor*, 1992]. Similar observations were also reported in Japan, with the mineral dust originating from China, and in the United States of America, with the mineral dust originating from Africa [*Prospero*, 1999]). The mass of soluble material on the mineral dust particles was found to be related to their surface area, suggesting that the deposition process could be surface dependent [*Levin et al.*, 1996; *Falkovich et al.*, 2001].

[4] The soluble coating of the mineral dust particles could significantly change their ability to serve as cloud

[1]School of the Environment, University of Leeds, Leeds, UK.
[2]Institute for Tropospheric Research, Leipzig, Germany.
[3]Department of Geophysics and Planetary Sciences, Tel Aviv University, Tel Aviv, Israel.
[4]Soreq Nuclear Research Center, Yavne, Israel.

0148-0227/02/2001JD001544$09.00

condensation nuclei (CCN). Evidence for the activation of these large CCN was observed at cloud base, where a few large drops containing both dust and sulfate were found [*Levin et al.*, 1996]. On the other hand, dust particles are relatively good ice forming nuclei (IFN), and coating them with soluble substances could affect their ability to act as IFN. Mineral dust can act as IFN by immersion freezing at temperatures of $\sim -9^{\circ}$C to -30°C depending on the chemical composition of the dust particles [*Pruppacher and Klett*, 1997], by contact freezing at temperatures $\sim -8^{\circ}$C, and by deposition nucleation at -15°C [e.g., *Meyers et al.*, 1992]. Coating them with soluble material may reduce the temperature of freezing due to the temperature depression of the solution if the drops are very small, but this effect is negligible at the larger drop sizes. Coating the dust with organics can change the picture completely, because some of the organics can act as surfactants which reduce the drop's ability to freeze. The ability of mineral dust, coated or uncoated, to act as IFN is a complex issue and these effects are not included in the present study. Ice formation in the model is only allowed to occur by vapor deposition (or condensation freezing), contact nucleation, and immersion freezing of supercooled drops, depending on the supersaturation and/or supercooling.

[5] There could be a number of pathways that could lead to the formation of sulfate-coated aerosol particles:

1. Formation of sulfate at the source region, as was suggested by *Falkovich et al.* [2001].
2. Heterogeneous reactions that could take place on the particles' surface in the presence of moisture.
3. Sulfate deposition on particles that interacted with clouds.

In this last mechanism the mineral dust particles are collected by cloud drops that have been originally nucleated by sulfate or other soluble aerosol particles. Additional sulfate is added by gas scavenging and subsequent liquid phase oxidation. In mixed phase clouds, mineral dust particles and drops can also be collected by ice particles. Melting of these ice particles contributes to the number of drops, which contain mineral dust and soluble materials. After cloud evaporation, mineral dust particles coated with soluble material and other cloud processed aerosol particles are released into the atmosphere.

[6] Numerical simulations, using a parcel model with detailed treatment of the microphysical processes [*Wurzler et al.*, 2000] have shown that the latter process of mineral dust-cloud interaction could lead to the increase of sulfate mass on the surface of the dust particles. It was also shown that increasing the number of times the particles had gone through clouds, increased the number of large particles that were coated with sulfate. The results of the parcel model also suggested that the cloud processed mineral dust particles could lead to an enhanced production of precipitation or drizzle sized drops. (The simulations were restricted to background mineral dust concentrations so the results might look different for a heavy dust storm situation). However, the use of a parcel model is limited by its neglect of sedimentation and its simplified dynamics. The effects of these coated particles on cloud macro-structure, ice formation and warm and cold precipitation development have not yet been studied.

[7] In recent years, much effort has been applied to understand the interactions between aerosol particles and clouds and their effects on the optical properties of the clouds. For example *Früh et al.* [2000] studied radiation effects in continental boundary layer clouds. *Feingold et al.* [1998] investigated the effects of cloud processing on the evolution of drops in stratiform clouds using large eddy simulations. They found that cloud processing could cause an increase or a decrease in drizzle formation, depending on the concentration of activated CCN.

[8] The effects of large cloud condensation nuclei on drizzle formation in marine stratocumulus clouds and their implications for cloud radiative properties were investigated by *Feingold et al.* [2000]. They found that both large and small CCN particles had a major impact on the formation of drizzle. Their results also indicated that the presence of giant CCN enhances the formation of drizzle drops and moderates the tendency of the numerous small CCN to make the cloud more continental. This tendency was also reflected in the calculated cloud optical properties.

[9] *Bott* [1995, 1996] and *Eichel et al.* [1996] have shown that not only the number and size of the CCN but also the distribution of the water soluble and water insoluble fractions of the aerosol particles significantly affect the microphysics of clouds and precipitation. The model simulations and sensitivity studies of *Flossmann* [1998] indicated that in a marine environment, varying the number of sulfate particles changed the number of cloud drops but had little effect on precipitation formation.

[10] On the other hand, numerical simulations of evolution of cloud and precipitation using an aerosol size distribution having a tail of large CCN or, alternatively, simulations of artificial cloud seeding with large hygroscopic particles [*Tzivion et al.*, 1994; *Reisin et al.*, 1996; *Yin et al.*, 2000a, 2000b; *Cooper et al.*, 1997], showed that in continental clouds, these large particles expedite the formation of large drops and enhance the efficiency of the collision-coalescence process. It is also found that the rapid growth of large drops enhances ice formation in colder convective clouds through the more efficient freezing of drops and through the Hallett-Mossop ice multiplication mechanism [*Hallett and Mossop*, 1974]. The efficient production of large drops and of ice particles modifies the time, the amount, and the distribution of the precipitation. However, the effect of the tail of the large particles on the rate and amount of precipitation in maritime clouds was only marginal.

[11] In this study, a two-dimensional cloud model with detailed description of warm and cold cloud microphysics is used to investigate the effects on cloud development due to changes in the CCN size distribution that occur due to cloud processing of aerosol particles and of coating of mineral dust particles with sulfate. The intention is to shed light on the microphysical and optical response of continental and maritime clouds to changes in the aerosol size and composition, especially to those that occur following a number of passes through clouds. The cloud processed aerosol particle spectra obtained with an entraining air parcel model by *Wurzler et al.* [2000] are used to initialize this model. This study is an improvement over past studies because in addition to the warm rain microphysical processes (as in the air parcel model), it also considers the ice phase

processes, which were absent in most of the previous studies.

2. A Brief Description of the Cloud Model

[12] The model is a two dimensional nonhydrostatic slab-symmetric cloud model with detailed description of the microphysics of warm and cold cloud processes. The wind components in the horizontal and vertical direction were calculated based on the stream function and the vorticity equation. The dynamic equations were also solved for the virtual potential temperature perturbation, the specific humidity perturbation, the concentration of CCN, the number and mass concentrations of each hydrometeor type considered (see *Yin et al.* [2000a] for more details).

[13] The warm microphysical processes included were nucleation of drops from CCN, condensation and evaporation, stochastic collision-coalescence, and binary breakup (Low and List kernel). Three different types of ice particles were considered: ice crystals, graupel particles and snowflakes (aggregates of ice crystals). The ice microphysical processes included were ice nucleation (deposition, condensation freezing, contact nucleation, and immersion freezing), ice multiplication (Hallett-Mossop mechanism), deposition and sublimation of ice, ice-ice and ice-drop interactions (aggregation, accretion and riming), melting of ice particles, and sedimentation of both drops and ice particles. All these microphysical processes were formulated and solved using the method of Multi-Moments [*Tzivion et al.*, 1987; *Reisin et al.*, 1996].

[14] The radius resolution of each hydrometeor type was given by 34 bins with mass doubling for adjacent bins. The mass of the lower boundary of the first bin and the upper boundary of the last bin for both liquid and solid phases were 0.1598×10^{-13} and 0.17468×10^{-3} kg, which correspond to hydrometeor equivalent diameters of 3.125 and 8063 μm, respectively. The aerosol particle spectrum was divided into 67 bins with a minimum radius of 0.0041 μm.

[15] The grid size of the model was set to 300 m in both horizontal and vertical directions (separate numerical tests using grid sizes of 150 and 200 m showed that except for a 2 min delay in the cloud and rain initiation, the development of cloud properties such as liquid water content, maximum updraft, ice content, were similar to those reported in this paper). However, it should be borne in mind that due to the relatively large spatial grid size used here, the small-scale turbulence observed in natural cloud is not properly resolved; therefore the size spectra of cloud and precipitation particles obtained in this study only represent gross averages over the grid boxes. The width and height of the domain were 30 and 12 km, respectively. The time step for all the processes was 5 s except for diffusive growth/evaporation, where a shorter time step of up to 2.5 s was used.

3. Initial Conditions

3.1. Aerosol Particles

[16] Two scenarios were studied: a continental and a pure maritime aerosol particle distribution. For the continental scenario, three aerosol spectra obtained from the results of an entraining air parcel model [*Wurzler et al.*, 2000] were used. These aerosol spectra represent three cycles through a cloud of an aerosol distribution including a tail of large mineral dust particles. The aerosol distribution reported by *Jaenicke* [1988] and the same spectrum of mineral dust particles were used for the maritime cases. The mineral dust particle concentrations used in both continental and maritime cases (about 10 l^{-1} of sizes between 0.1 and 10 μm) correspond to those found in small dust storms [e.g., *Levin et al.*, 1980]. It was also assumed that the mineral dust particles without a soluble coating cannot be activated to drops. The ability of mineral dust particles to be activated as IFN was not included in the present study.

Table 1. Parameters for the Aerosol Particle Distributions[a]

	Mode i	n_i	R_i	log σ_i
CO	1	350	0.028	0.15
	2	459	0.06	0.17
	3	50	0.1	0.21
	4	30	1.2	0.3
C1	1	350	0.028	0.165
	2	459	0.06	0.17
	3	35	0.1	0.35
	4	620	0.105	0.1
	5	2	0.8	0.45
C2	1	6050	0.024	0.39
	2	350	0.028	0.165
	3	459	0.06	0.17
	4	620	0.09	0.1
	5	60	0.11	0.65
	6	2.5	2.0	0.45
M0	1	133	0.0039	0.657
	2	66.6	0.133	0.21
	3	3.06	0.29	0.396
	4	30	1.2	0.3
M1	1	133	0.0039	0.657
	2	66.6	0.133	0.21
	3	3.06	0.29	0.396
	4	5.86	0.25	0.1
	5	2.93	0.15	0.25
	6	0.00234	4.5	0.27
	7	30	1.2	0.3
M2	1	133	0.0039	0.657
	2	66.6	0.133	0.21
	3	3.06	0.29	0.396
	4	19.05	0.3	0.17
	5	5.86	0.15	0.27
	6	0.00023	12.0	0.25
	7	30	1.2	0.3

[a] n_i = total number of aerosol particles per cubic centimeter of air, R_i = geometric mean aerosol particle radius in μm, σ_i = standard deviation in mode i.

[17] The aerosol distributions obtained from the air parcel model after cloud evaporation from the first and second cycles were used to initialize the clouds in the second and third cycles in this study, respectively. From here on, the first, second and third cycles will be referred as C0, C1 and C2 for the continental cases, and M0, M1 and M2, for the maritime cases.

[18] These aerosol distributions were fitted by superimposing four, five, and six log-normal distributions [*Jaenicke*, 1988], for the continental cases C0, C1 and C2, respectively, and four and seven log-normal distributions for the maritime cases M0, M1 and M2. The parameters of the distributions are given in Table 1. Figure 1 shows the number density distributions of the aerosol particles (only the soluble fractions) used in the continental and maritime cases. The concentrations of particles were assumed to decrease exponentially with height with a scale height of 2 km. Following

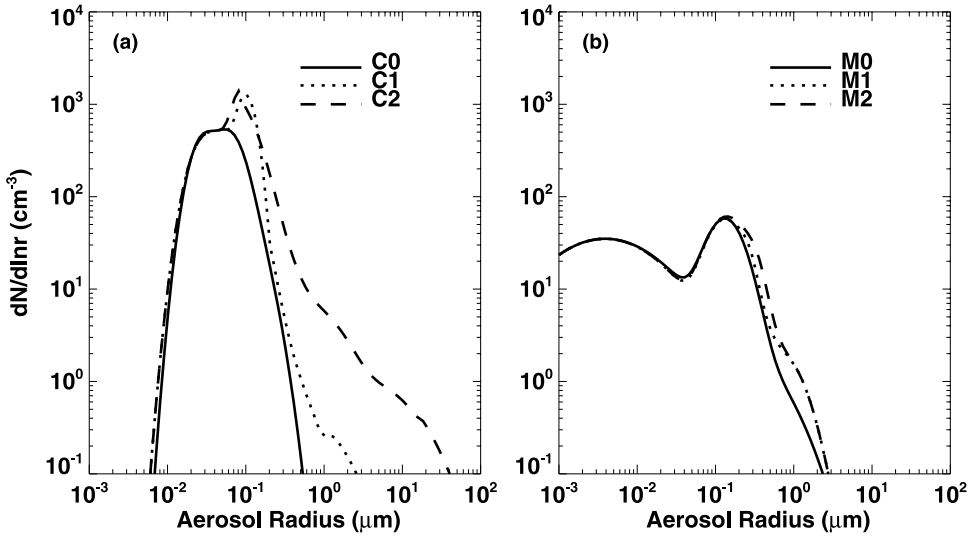

Figure 1. Number distributions of the initial aerosol particles (soluble fraction) as a function of particle radius for (a) the continental cases C0, C1 and C2, and (b) the maritime cases M0, M1 and M2.

Hatzianastassiou et al. [1998], particles larger than 10 μm in radius were removed, before introducing these aerosol spectra into the two dimensional model, to correct for the sedimentation process disregarded in the parcel model. Further numerical experiments with a tail of ultragiant particles ($r > 10$ μm) being included showed that the precipitation development in the second and third cycles of the continental cloud was initiated earlier and produced slightly larger amounts of precipitation. Since the differences between the runs with and without these ultra giant particles were small and since the parcel model cannot adequately describe their lifetime, we omitted the use of these ultragiant particles from the simulations in this paper.

[19] Note that in the atmosphere the cloud processed aerosol particles undergo mixing or dilution with the aerosol particles in the ambient air. This effect was not included in the present study. It was assumed that the subsequent clouds would form directly on the aerosol particles released by the previously evaporating cloud. Therefore this study should be interpreted as a sensitivity study of the effects of coated mineral dust particles on clouds. In both C0 and M0 it was assumed that none of these particles were present whereas in the subsequent clouds increasing numbers of coated mineral dust particles were available as CCN. The real effects of coated mineral dust particles and other large CCN on clouds will therefore be somewhere between the results obtained in C0 and M0 (none of them present) and C2 and M2 (many giant CCN), respectively.

3.2. Thermodynamic Conditions

[20] The initial thermodynamic conditions for all reported cases were given by theoretical profiles of temperature and dew point temperature as shown in Figure 2. These thermodynamic profiles represent the average initial thermodynamic conditions of summer convective clouds [e.g., *Krauss et al.*, 1987; *Cooper and Lawson*, 1984] with cloud base at 8–10°C and top at −25°C. For initialization, a pulse of heat that produced a 2°C perturbation was applied for one time step at $t = 0$ at one grid point at a height of 600 m, at the middle of the domain. Therefore the clouds initialized in this study only depend on the instability of the atmosphere, not on the area of the initial disturbance. The possible influence of wind shear was not considered.

4. Results

4.1. General Features of the Clouds

[21] The time evolution of the maximum updraft velocities were quite similar in both the continental and maritime cases, as can be seen from Figure 3. For the first 28 min an almost constant updraft velocity resulted from the initial impulse. The increase in updraft velocity after that time stems from the onset of condensation and the release of

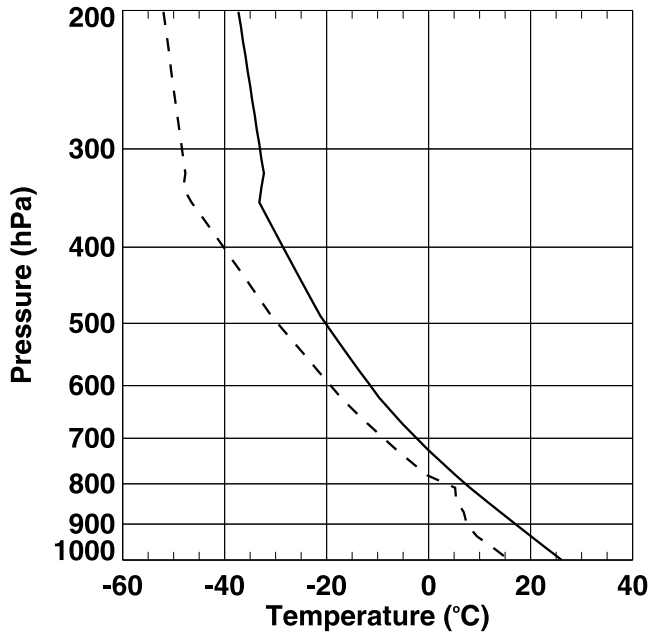

Figure 2. Initial vertical profiles of temperature (solid line) and dew point temperature (dashed line) used in the present work.

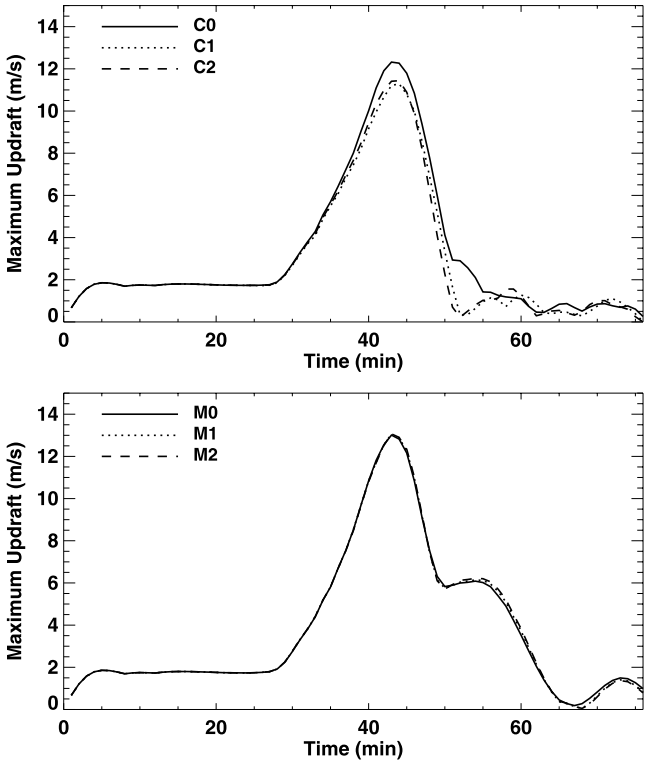

Figure 3. Time evolution of maximum vertical velocity at the main updraft core in the continental (C0, C1, and C2) and maritime (M0, M1 and M2) cases.

latent heat, with the highest condensation rate at around 40 min. The vertical velocity was further enhanced by the latent heat release produced by the onset of ice formation. The decrease in the maximum updraft velocities after 40 min was caused by the falling precipitation particles, their mass loading and the cooling due to their evaporation and melting. The differences in the maximum updraft velocities in the time interval of 50–60 min among the continental cases resulted from the differences in the precipitation behavior of the clouds, which will be shown later. The secondary peak in the maritime cases after 50 min of simulation was a consequence of increased buoyancy due to the relatively strong release of latent heat, as compared to the continental cases, during drop freezing and coagulation between drops and ice particles.

[22] In all the continental and maritime cases cloud droplets formed after approximately 23 min of modelling time, as can be seen from the time evolution of the maximum liquid water contents (LWC) and number concentrations of the drops shown in Figure 4. The relatively long time for cloud initialization was related to the small area of initial disturbance as described in the previous section. Figures 5a and 5b shows the spatial distributions of mixing ratio and number concentration of drops, ice crystals, and graupel particles, 2-D wind field and temperature in cases C0, C1 and C2 after 44 and 52 min of simulation (these correspond to the times at which the maximum LWC and maximum graupel production appeared, respectively). As a consequence of the initial temperature and humidity profiles all cloud bases were located at a height between 1.5 and 1.8 km (T $\approx$ 8–10°C) and the tops

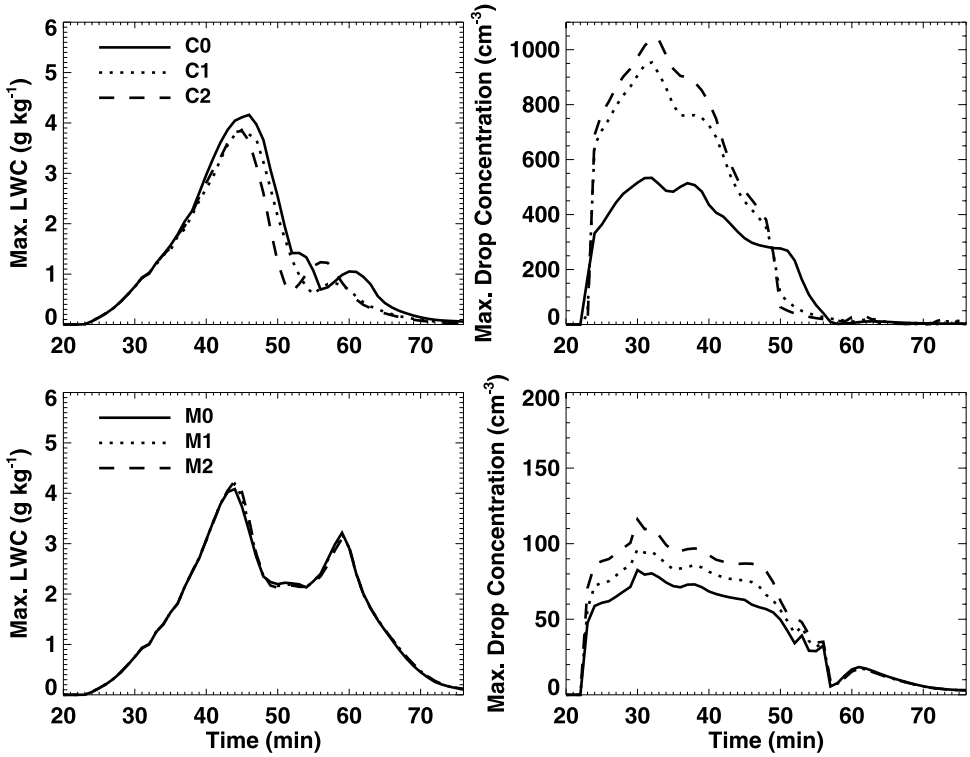

Figure 4. Time evolution of maximum liquid water contents (LWC) and number concentrations of drops at the main updraft core in the continental cases C0, C1 and C2.

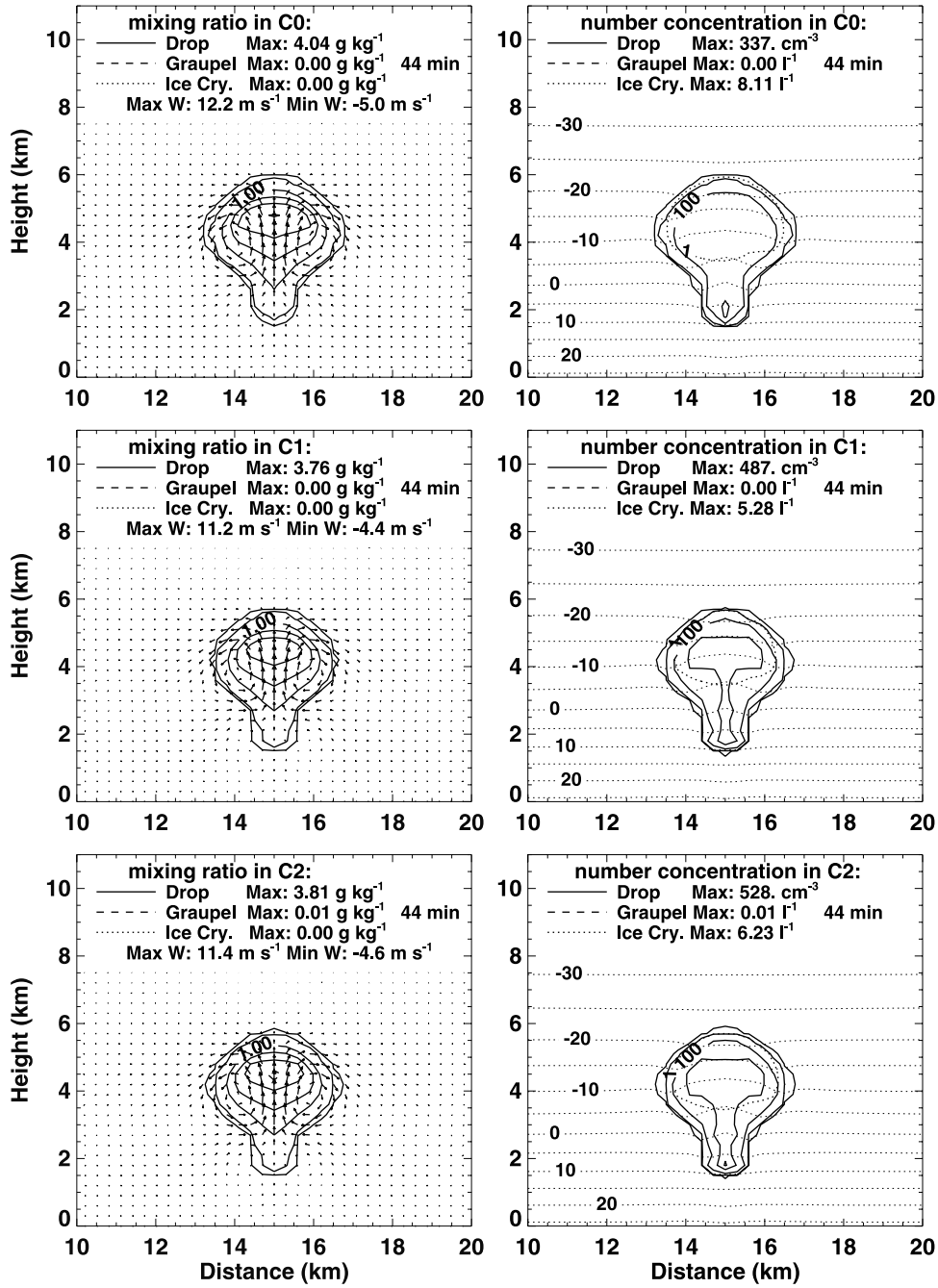

Figure 5. Spatial distributions of mixing ratio (left panels) and number concentration (right panels) for drops, graupel and ice crystals, (a) and wind vectors at the peak cloud water developing stage (44 min), and (b) around the maximum developing time for graupel (52 min) in the continental case. The horizontal dotted lines are isotherms. The contour values are 0.01, 0.1, 1, 2, 3, and 4 g kg^{-1} for mixing ratio; 1, 10, 100, 300, and 500 cm^{-3} for drop number concentration; 1, 10, 20, 30 l^{-1} for number concentration of ice crystals; and 0.1, 1, 3, 5 for number concentration of graupel particles.

of the fully developed clouds reached a height between 6.5–7 km (T ≈ -25°C).

[23] From Figure 4 it can be seen that although the maximum liquid water contents were similar in C0, C1 and C2, the maximum drop number concentration in C0 was much lower than those in C1 and C2. This is due to the smaller aerosol number concentration in C0 as compared to the other two cases (see Figure 1). Similar characteristics are also found in the three maritime cases M0, M1 and M2, although the maximum drop concentrations were much lower than those in the continental cases. The secondary peak in the maximum LWC in the maritime cases around 60 min was caused by convergence of LWC because of the heavier precipitation.

[24] Ice crystal formation started in all continental and maritime cases after 34 min of simulation but the concen-

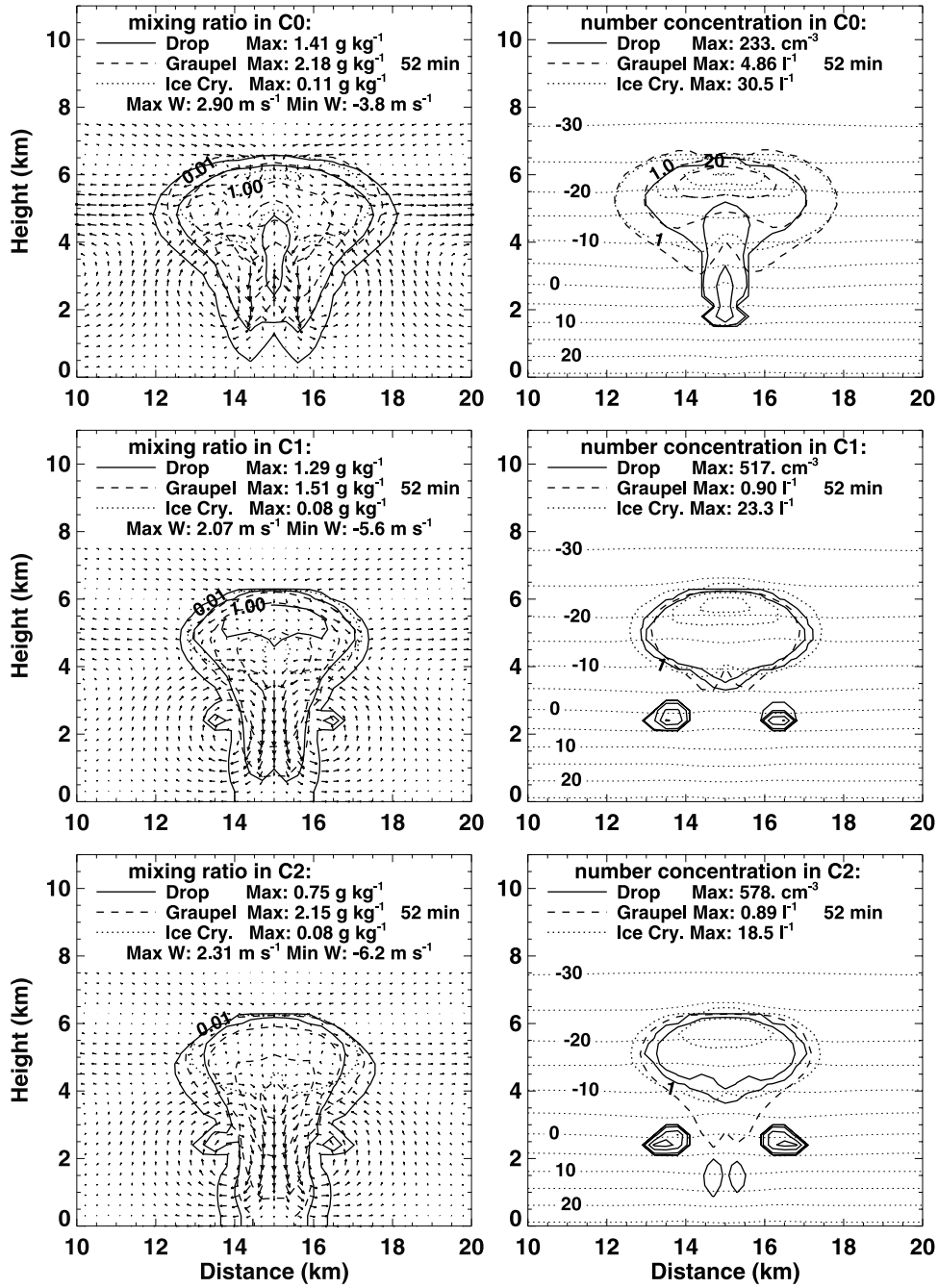

Figure 5. (continued)

trations remained relatively small prior to 40 min (see Figure 6). After 40 min the concentrations of ice crystals in all cases increased very rapidly and reached their peak values around 50 min. Figure 6 also shows that the number concentration was higher in case C0 than those in C1 and C2. This can be explained by examining the various microphysical processes responsible for ice production in these cases. Table 2 shows the maximum rates of various ice formation processes in all the cases at selected times. It can be seen that in the continental cases, vapor deposition and condensation freezing dominated the ice formation before 48 min, and thereafter, immersion freezing of drops became the most important process. The higher production rate for ice crystals prior to 44 min in C0 was mainly related to the relatively higher supersaturation with respect to ice as compared to C1 and C2. This is because C0 had the lowest drop concentration of the three cases, the competition of drops for available water vapor in this case was not as strong as that in the other two cases. At 40 min, for example, the supersaturations with respect to ice in C0, C1 and C2 were 15.8%, 13.7%, and 13.7%, respectively. After 48 min, immersion freezing process contributed most to the production of ice crystals (by droplets smaller than 100 μm in diameter) and graupel particles (by droplets larger than 100 μm in diameter). At 48 min, the rate of ice formation in C0 was more than twice that in cases C1 and C2.

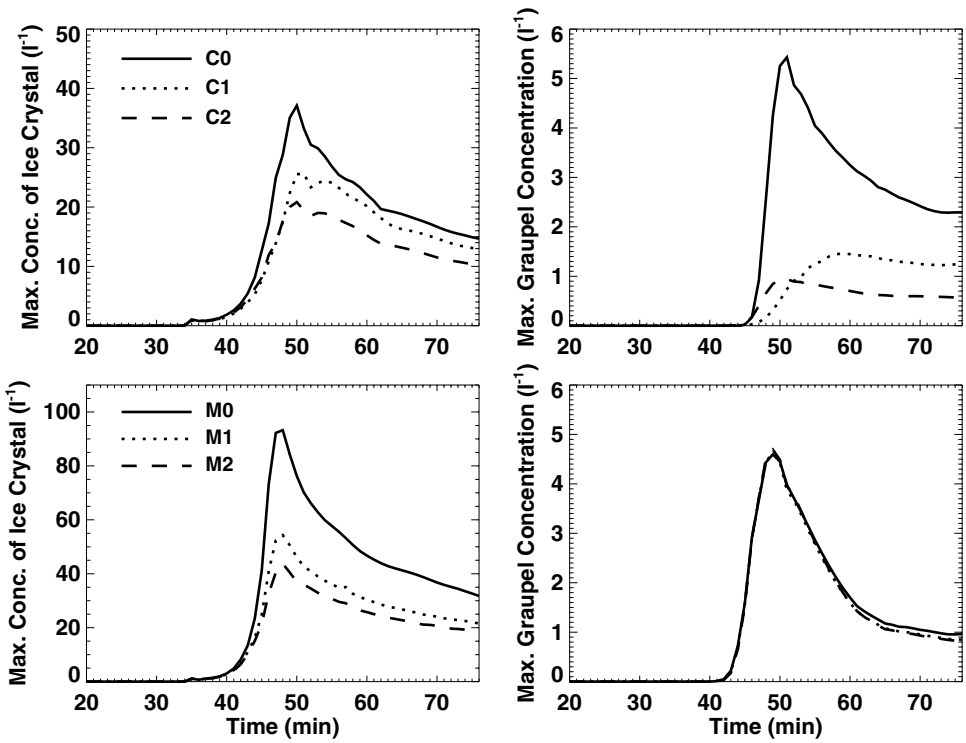

Figure 6. Time evolution of maximum concentrations of ice crystals and graupel particles at the main updraft core in the continental cases C0, C1 and C2 (top), and the maritime cases M0, M1, and M2 (bottom).

Table 2. The Maximum Rate (In Number Per Cubic Meter Per Second) for Ice Formation Via Various Microphysical Processes at Selected Times (Minutes of Simulation)

Cases	Features	36	40	44	48	52	56	60
CO	Imfr	0.001	0.161	19.11	263.5	20.34	1.78	0.545
	Depo	9.14	122.3	55.68	49.15	–	–	–
	Cont	–	0.003	–	0.001	–	–	–
	Mult	–	–	–	–	0.391	0.005	–
	Gcol	–	–	0.006	3.07	2.59	0.94	0.329
C1	Imfr	0.001	0.824	8.0	125.3	48.39	8.97	3.12
	Depo	12.46	18.76	112.7	48.53	6.524	7.75	–
	Cont	–	0.018	–	–	–	–	–
	Mult	–	–	–	0.005	–	–	–
	Gcol	–	–	0.02	0.687	2.10	2.43	1.19
C2	Imfr	0.001	0.089	11.62	102.5	19.6	5.52	1.41
	Depo	8.35	23.52	102.6	25.49	7.63	3.81	4.98
	Cont	–	0.004	–	–	–	–	–
	Mult	–	–	–	0.053	–	–	–
	Gcol	–	–	0.141	1.19	0.721	0.455	0.219
MO	Imfr	0.002	0.291	34.22	90.42	9.32	1.0	1.37
	Depo	–	108.9	824.9	717.3	266.3	318.1	91.93
	Cont	–	–	0.002	–	–	–	–
	Mult	–	–	–	0.042	0.029	0.040	–
	Gcol	–	0.034	4.94	5.16	1.13	0.357	0.435
M1	Imfr	0.002	0.295	35.72	98.11	9.18	0.99	2.646
	Depo	–	88.57	648.4	359.0	128.6	196.2	56.43
	Cont	–	–	–	–	–	–	–
	Mult	–	–	–	0.098	0.050	0.116	–
	Gcol	–	0.019	3.40	3.12	0.795	0.297	0.189
M2	Imfr	0.002	0.296	36.67	99.3	8.51	1.26	3.28
	Depo	–	81.05	609.1	277.8	88.9	172.2	49.46
	Cont	–	–	0.001	–	0.003	–	–
	Mult	–	–	–	0.127	0.057	0.136	–
	Gcol	–	0.011	2.84	2.79	0.746	0.289	0.142

[a]The nomenclature of the features is as follows: Imfr, immersion freezing; Depo, deposition and condensation freezing; Cont, contact nucleation; Mult, ice multiplication; and Gcol, production of graupel by coagulation of ice particles and drops. The values smaller than 10^{-3} are not shown.

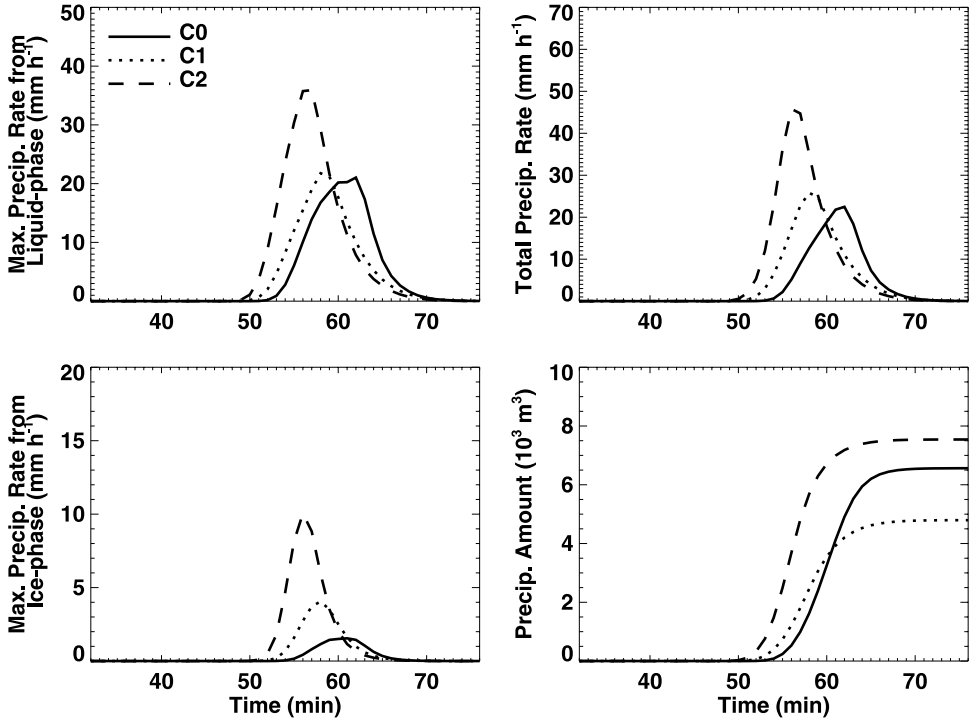

Figure 7. Time evolution of precipitation rate from liquid phase, ice phase, and the total condensate, and integrated precipitation amount in cases C0, C1 and C2. When the integrated precipitation amount is calculated, the width of the precipitation area in y direction is normalized to 1 km.

[25] In contrast to the continental cases, vapor deposition and condensation freezing dominated the ice formation throughout the lifetime of the maritime clouds. The lower droplet concentration in these cases, as compared to the continental cases, led to higher supersaturations, and Therefore higher production of ice crystals by deposition nucleation. Once again, M0, which was unaffected by processed aerosol particles and by mineral dust particles, had the highest rate of ice crystal production of the three cases.

[26] Graupel particles began to form at 46 min in C0 and C1 and at 44 min in C2. The maximum graupel concentrations in C0, C1 and C2 were 6.4, 1.5, and 1.0 l^{-1}, respectively. In the maritime cases, graupel particles began to appear at 44 min and the peak concentrations were similar ($\sim$5.0 l^{-1}) in all cases. The earlier appearance of graupel particles in C2 as compared to the other two continental cases is related to the earlier formation of large drops, which will be discussed in detail in the following section. Graupel particles were formed mainly by freezing of large drops (diameter larger than 100 μm in this study), and by coagulation between drops and ice particles. From Table 2 one sees that both of these processes had a larger production rate of graupel particles in C0 than in C1 and C2 during the main ice phase development stage (44–52 min). On the other hand, the differences in freezing rate among the three maritime cases M0, M1, and M2 are much smaller, which led to very similar graupel production in these cases.

[27] Figure 7 shows the time evolution of the precipitation from the continental clouds. The onset of precipitation in C0 was approximately 4 min later than in C1 and C2. Whereas from C0 most of the precipitation which reached the ground consisted of drops, part of the precipitation from C1 and C2 contained ice-phase (mainly graupel) particles as can be seen from Figure 7. The sizes of the ice particles in C1 and C2 were larger than those in C0 (for reasons described later), so fewer of them melted completely on their way to the ground.

[28] The cloud formed in C1 produced significantly less rain than that in C2. The results of C1 and C2 represent a competition between the effects of the increased continentality of the clouds due to the increase in small CCN and the effect of the added large and giant CCN, as compared to the initial aerosol particle distribution in C0 (see Figure 1). In both C1 and C2 the cloud-processed aerosol and dust particles increased the total CCN concentration and nucleated more drops than in C0. It is also seen from Figure 7 that precipitation is accelerated due to the inclusion of giant CCN that formed by cloud processing of dust particles. The precipitation efficiency is increased in C2 as compared to C1 because of the higher concentration of such giant CCN in the former case. It is therefore clear that the effect of increasing the giant CCN that enter C2, far outweighs the effects of increasing the total drop numbers due to the higher concentrations of small CCN that enter the same cloud.

[29] The time evolution of the precipitation in the maritime cases is shown in Figure 8. Compared to the continental cases discussed above, the difference in precipitation between the three maritime cases M0, M1 and M2 was much smaller, in spite of the fact that the total number of CCN and cloud drops were higher in M1 and M2 than in M0. It seems that adding giant CCN to clouds that already had similar size

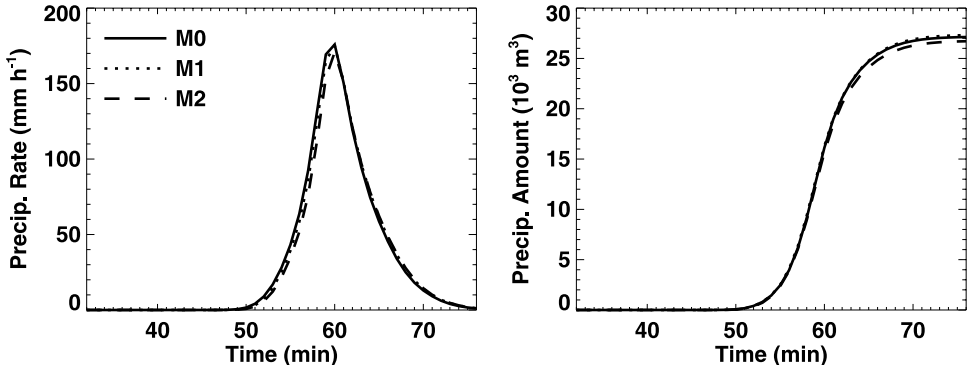

Figure 8. Time evolution of precipitation rate and integrated precipitation amount in cases M0, M1 and M2. When the integrated precipitation amount is calculated, the width of the precipitation area in y direction is normalized to 1 km.

nuclei, produced very little effect on the development of precipitation.

4.2. Analysis of the Size Distributions of Hydrometeors

4.2.1. Continental Clouds

[30] The time evolution of the mass and number distribution functions of drops at two different altitudes in the continental clouds are shown in Figures 9a and 9b. From Figure 9a it can be seen that the droplets formed at the lower region of the cloud (2100 m) in the early growth stages in C0 were smaller than those in C1 and C2. This is due to the relatively narrow initial aerosol particle spectrum in C0, in which all the dust particles were assumed to be water-insoluble and remained interstitial. In case C1 and C2 a portion of the dust particles that were coated with water-soluble components, produced higher concentrations and broader size distributions of drops. This is especially noticeable in C2. These results are in agreement with those from the parcel model simulations [*Wurzler et al*. 2000].

[31] The formation of the broader size spectra in C1 and C2 accelerated the formation of precipitation by collision-coalescence process. As can be seen in Figure 7, the rain from these two clouds started earlier than in C0. This is because precipitation size particles in these clouds appeared earlier and closer to cloud base (see also Figure 9a). It should also be noted that the amount of rain falling from C1 was smaller than that from C0. This is in contrast to the much larger rain amount falling from C2. This is because the added CCN particles (cloud processed aerosol and mineral dust particles coated with sulfate) to C1 were primarily in the small size range (0.1–0.4 μm), as seen in Figure 1. These particles produced more small drops with

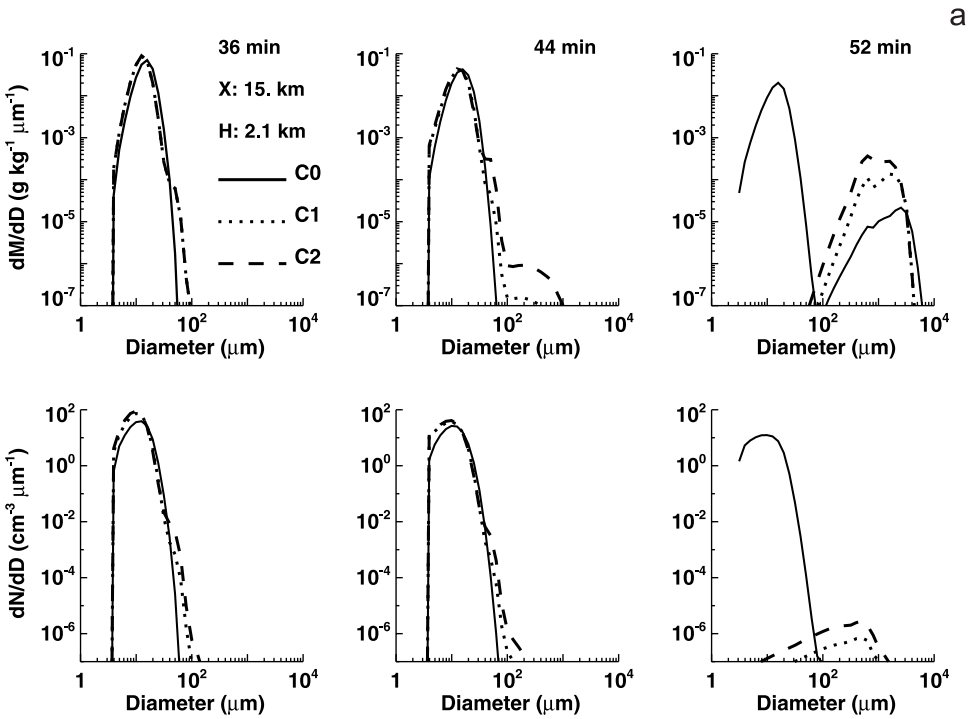

Figure 9. Drop mass (top) and number (bottom) distribution functions at (a) 2100 m, and (b) 6000 m height at different times in cases C0, C1 and C2.

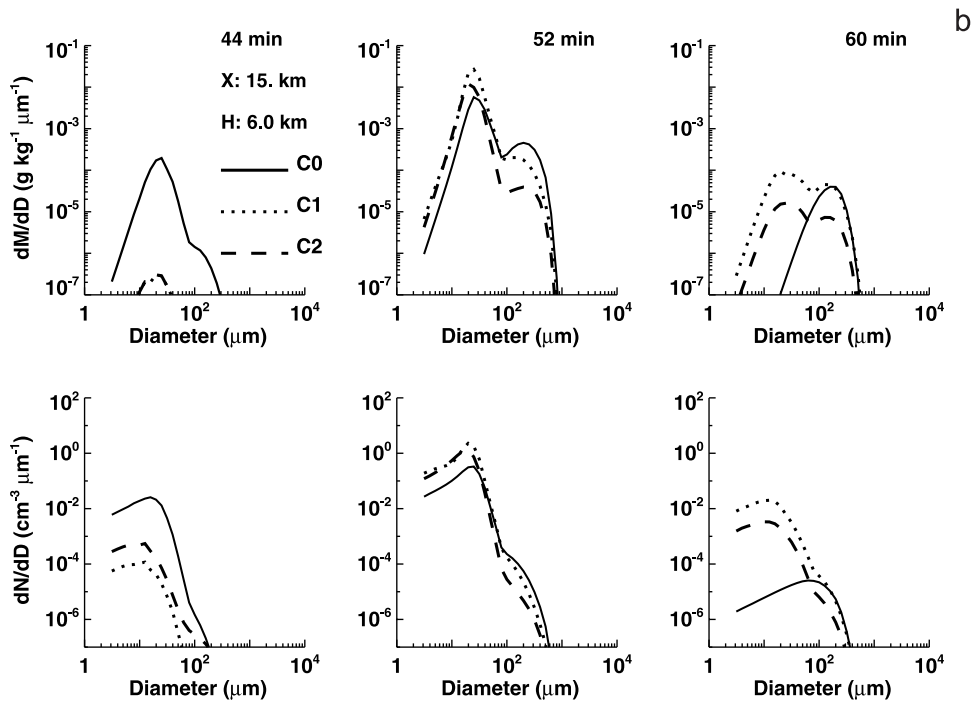

Figure 9. (continued)

only a few large ones (0.8–2 μm). These few large particles grew to precipitation size and fell early, thus initiating the early rainfall. However, since their number was relatively small, their contribution to the total rainfall amount was small either. On the other hand, the increased number of CCN in the smaller sizes ($r < 0.4$ μm) produced much higher concentration of small drops that reduced the formation of precipitation. In the "tug of war" between the effects of the increased concentration of small CCN versus the large ones, the smaller ones won in C1. On the other hand, in C2 the number of giant CCN particles increased significantly, even to the point of producing particles as large as 20 μm. In this case the production of precipitation increased dramatically far above the effects of the smaller particles (see Figure 7).

[32] The mass and number distribution functions of the droplets in cases C0, C1 and C2 at the upper region of the clouds (6000 m height) are shown in Figure 9b. From this figure one sees that prior to 48 min larger numbers of small drops were lifted into the upper layer in C0 than in the other two cases. But after that time, especially at the mature and dissipation stages of the cloud, many more small droplets in C1 and C2 than in C0 were present at the upper cloud layer. These differences could lead to significant changes in the cloud optical properties, as seen from above, and will be further discussed in the next section. The higher concentration of small droplets in the upper layers in C1 and C2, as compared to C0, was caused by two effects: the larger number of CCN (small and large) in C1 and C2 and the early fallout of precipitation particles from lower levels of the clouds (Figure 9a), leaving the uncollected small drops and ice crystals suspended at the upper reaches of the clouds. The difference between case C2 and C1 is due to the relatively higher concentration of giant CCN in the former than in the latter. This resulted in more efficient precipitation formation in C2, and helped to deplete more of the smaller drops in this case. This in turn, reduced the number of such drops that reached the upper parts of the cloud.

[33] Compared to the differences in drop size distributions among C0, C1 and C2, the differences in distributions of ice crystals were much smaller, but the differences in graupel production were significant. An analysis of graupel production reveals that the cloud in C2 was the first to produce graupel particles, followed by C1 and C0. This result is consistent with the findings of *Yin et al.* [2000a] that the giant CCN, most of which are present in C2, not only accelerated the rain drop formation via collision-coalescence process, but also promoted the production of ice-phase precipitation through drop freezing and subsequent collection of drops and ice particles. The reason for this behavior is that the drop freezing process is very sensitive to drop size [e.g., *Bigg*, 1953]. Once being lifted up to the freezing layers, the larger drops would freeze first. In addition, these large drops have a higher efficiency to impact ice crystals which would help initiate the freezing process. However, the advantage of C2 over the other cases in producing graupel particles disappeared after 52 min. At that point the concentration of the graupel particles in C0 exceeded that in C1 and C2 (also seen from Figure 6).

4.2.2. Maritime Clouds

[34] The general features discussed above for the continental clouds are also valid for the maritime clouds, but the differences in development of distributions of hydrometeors and precipitation among these cases are much smaller than those in the former cases. This is in agreement with the results of *Flossmann* [1998], who found no difference in the precipitation behavior of maritime clouds due to an increase in sulfate particles. Similar conclusion was also

reached by *Yin et al.* [2000a] for mixed-phase clouds. Although clouds in cases M0, M1 and M2 displayed no significant differences in the precipitation behavior and also no major differences in the graupel formation, there are considerable differences in the drop number concentrations and the concentrations of ice crystals between these cases (see Figure 6).

4.3. Effects on Cloud Optical Properties

[35] The optical properties of clouds affected by dust particles that had previously interacted with clouds were estimated by calculating the cloud optical depth and the albedo. The cloud albedo A has been approximated by

$$A \approx \frac{(1-g)\tau}{2+(1+g)\tau}, \tag{1}$$

[*Bohren*, 1987], where, g is the asymmetry factor ($\approx$0.84), τ is the cloud optical depth (in the visible) and is given by

$$\tau \approx \int_{z_b}^{z_t} \int_0^{\infty} 2\pi r^2 n(r) dr dz, \tag{2}$$

where $n(r)$ defines the spectra of hydrometeors with radius/equivalent radius r for drops/ice particles, z_b is cloud base, z_t is cloud top. It should be noted that ice particles are not spherical. Treating them as spheres in the calculations for the radiative properties leads to underestimation of their effects. In reality, the cross section of the ice particles is larger, giving rise to larger effective radius. Also the asymmetry factor g is smaller, leading to increased albedo. But in the present simulations the upper parts of the clouds contain both ice crystals and water drops. Therefore the interaction between the particles and the solar radiation is much more complex. Since the present paper focuses mainly on the differences between maritime and continental clouds and since the results show that the role of water drops in the development of precipitation is more important than that of the ice crystals, the effects of the nonsphericity of the ice particles is expected to be similar in both simulated continental and maritime clouds. A more accurate calculation would need to include the effects on radiation due to changes in the particle shape with temperature and the changes in their size with supersaturation. These effects will be dealt with in a future paper. As can be seen the optical depth is affected by the changes in concentration and size of the cloud particles (drops and ice crystals). Increase in drop concentrations due to increase in CCN will result in larger optical depth. Similarly it will increase the cloud albedo.

[36] Figure 10 shows the time evolution of cloud optical depth, τ and albedo, A in the three simulated continental clouds in cases C0 and C1 and C2. From this figure one can see that τ and A values are smaller in C0 than in the other two cycles during the developing stage (before 44 min) and during the dissipating stage (after 52 min). Between 44 and 52 min τ and A in C2 are the lowest of the three cases. As has been discussed above, this resulted from the earlier development of large drops by collision-coalescence and graupel particles by coagulation of drops and ice particles, leading to depletion of more small drops

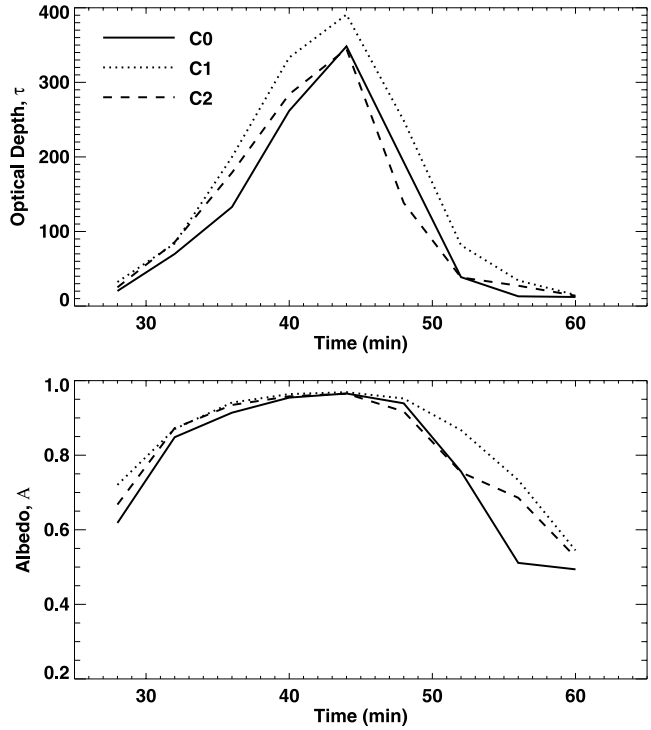

Figure 10. Time evolution of the cloud optical depth and albedo in cases C0, C1 and C2.

at the lower levels in C2 and to a lesser extent also in C1. Consequently, the cloud optical depth and albedo in C2 decreased. The small cloud particles in C0 continued to rise and grow. Precipitation began to fall from higher levels, depleting many of the small cloud particles closer to cloud top. This led to a decrease in the cloud optical depth and albedo (after 52 min), to levels even smaller than in the other two cycles.

[37] The larger values of τ and A in C1 and C2 as compared to that in C0 (except for the period between 44 and 52 min for C2), are a net effect of higher concentration of droplets and lower concentration of ice crystals. The results indicate, at least in these cases, that the role of the cloud droplets is more significant than that of the ice crystals in determining the optical depth and albedo of the clouds. These results are in contrast with the Arctic stratus simulations of *Jiang et al.* [2000] and *Harrington et al.* [1999] where pronounced sensitivities to the optical properties of clouds was found for the ice phase. This is because in those papers the low liquid content clouds glaciated readily while the clouds in this study do not.

[38] The time evolution of cloud optical depth, τ and albedo, A in the three simulated maritime cases M0, M1 and M2 is given in Figure 11. This figure shows that the clouds affected by the aerosol and mineral dust particles passing through earlier cloud cycles (M1 and M2) produced higher values of cloud optical depth and albedo than the cloud (M0) that developed in the pure maritime environment. This is consistent with the differences in the time evolution of droplet concentrations in the clouds (Figure 4), but is inconsistent with the evolution of the ice crystals. Once again, this indicates that the concentration and distribution of cloud droplets in these cases contributed most to the

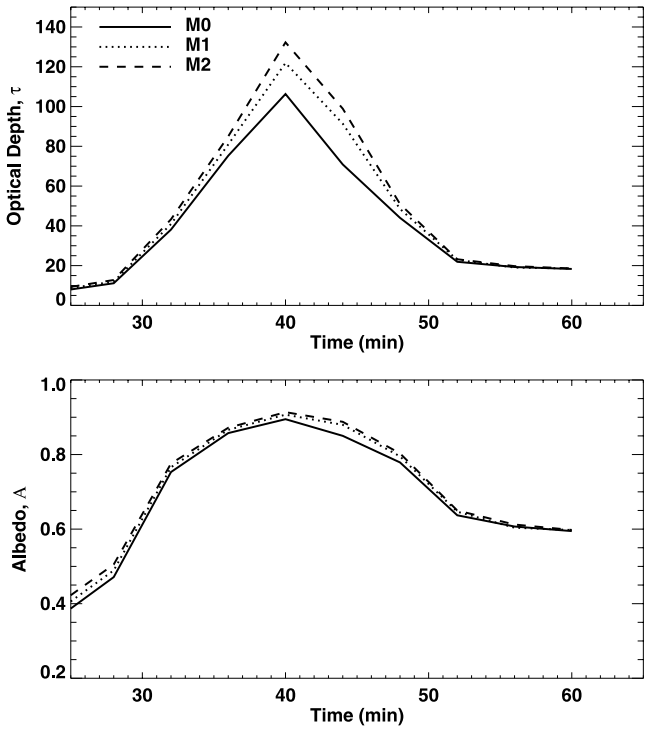

Figure 11. Time evolution of the cloud optical depth and albedo in cases M0, M1 and M2.

cloud optical properties, under the assumption that all cloud particles are spherical.

5. Discussion and Conclusions

[39] The study of *Wurzler et al.* [2000] shows that the interaction of insoluble mineral dust particles with clouds modifies the composition and size of the particles that are eventually released into the atmosphere following cloud evaporation. Many of these particles become coated with soluble sulfate, converting them into efficient CCN. The more times these particles go through clouds, the larger the mass of soluble material they accumulate. The present study shows that the ingestion of these newly formed or modified particles into other clouds influences the development of precipitation and the optical properties in them, especially in continental clouds. In fact the introduction of these aerosols into the clouds have two competing effects. The large particles acting as giant CCN, produce larger drops which tend to rapidly form precipitation by collecting small drops formed on the large number of small CCN particles. At the same time, the larger concentrations of drops, be they large or small, compete for the available water vapor. In this case, the drops may be smaller, reducing the efficiency of precipitation development [*Feingold et al.*, 1998; *Yin et al.*, 2000b; *Rosenfeld et al.*, 2001]. This effect can be seen when one compares the clouds in C0 and C1. In C1 the increase in the concentrations of the large and giant CCN indeed accelerated the formation of rain, but the larger increase in the number of small CCN particles caused the total net rainfall to be lower. As the concentrations of giant CCN increases like in C2, the added large particles produces an added amount of rain so that the total rainfall amount becomes larger (compare C1 and C2). In contrast, when the total concentration of CCN is small or when the ratio of large to small CCN is large, such as in the maritime cases (M0, M1 and M2), the efficiency of precipitation development is high to begin with [see also *Yin et al.*, 2000a] and the addition of more small CCN will tend to reduce the total rainfall. It turns out that the added giant CCN in this case, cannot compensate for the negative effect of the added small ones. Therefore there must be a point between these two extremes in which the two effects just balance each other. The maritime situations M0, M1 and M2 come relatively close to the point of balance between the increase of small CCN and the increase of large and giant CCN.

[40] These effects are also apparent in the optical properties of the clouds. The optical depth, which is an indication of the particle concentration near cloud top shows that those clouds that have high efficiency of rain formation have lower optical depth. The present study shows that in both the continental and maritime cases, clouds affected by aerosol and mineral dust particles passing through former cloud cycles produced higher cloud optical depth and albedo, and that, with the assumption that all cloud particles are spherical, the changes in these optical properties are mainly caused by the changes in concentration and distribution of cloud droplets, instead of those of ice crystals.

[41] However, it should be borne in mind that in the atmosphere the cloud processed aerosol particles would undergo mixing or dilution with the aerosol particles in the ambient air. This effect was not included in the present study. The assumption of spherical ice particles may also restrict the generality of the results. Nevertheless, the numerical simulations conducted in this study show that in continental clouds the effect of cloud-processed dust particles is to accelerate the formation of rain, and the amount of rain depends on the concentration of the large and giant CCN. In maritime clouds, the addition of cloud-processed aerosol and mineral dust particles has a minimal effect on precipitation, because the cloud starts with many large particles already. The addition of more CCN to either maritime or continental clouds increases their optical depth, even for those cases in which the rainfall is increased.

[42] **Acknowledgments.** One of the authors (S.Wurzler) acknowledges the BMBF (AFS program, project 07AF214/9) for providing funding for the present study. Parts of this work were carried out under the sponsorship of the German-Israeli Foundation under contract I-544-156.08/97. The comments and suggestions by two anonymous referees helped us clarify some of the important points and improved the quality of this paper. We thank them for that. The information about calculation of cloud radiative properties provided by Dr. Steve Dobbie (University of Leeds, UK) is also highly appreciated.

References

Bigg, E. K., The formation of atmospheric ice crystals by the freezing of droplets, *Q. J. R. Meteorol. Soc.*, *79*, 510–519, 1953.

Bohren, C. F., Multiple scattering of light and some of its observable consequences, *Am. J. Phys.*, *55*, 524–533, 1987.

Bott, A., The impact of the physico-chemical microstructure of atmospheric aerosols on the formation of stratiform clouds, *J. Aerosol Sci.*, *26*, S889–S890, 1995.

Bott, A., A microphysical model for the cloud topped boundary layer, in *Proceedings of the 12th International Conference on Clouds and Precipitation, Zürich*, pp. 725–728, Page Bros., Norwich, Ct., 1996.

Cooper, W. A., and R. P. Lawson, Physical interpretation of results from the HIPLEX-1 experiment, *J. Clim. Appl. Meteorol.*, *23*, 523–540, 1984.

Cooper, W. A., R. T. Bruintjes, and G. K. Mather, Some calculations pertaining to hygroscopic seeding with flares, *J. Appl. Meteorol.*, *26*, 1449–1469, 1997.

Eichel, C., M. Krämer, L. Schütz, and S. Wurzler, The water-soluble fraction of atmospheric aerosol particles and its influence on cloud microphysics, *J. Geophys. Res.*, *101*, 499–510, 1996.

Falkovich, A. H., E. Ganor, Z. Levin, P. Formenti, and Y. A. Rudich, Chemical and mineralogical analysis of individual mineral dust particles, *J. Geophys. Res.*, *106*, 18,029–18,036, 2001.

Feingold, G., S. M. Kreidenweis, and Y. Zhang, Stratocumulus processing of gases and cloud condensation nuclei, 1, Trajectory ensemble model, *J. Geophys. Res.*, *103*, 19,527–19,542, 1998.

Feingold, G., W. R. Cotton, S. M. Kreidenweis, and J. T. Davis, The impact of giant cloud condensation nuclei on drizzle formation in stratocumulus: Implications for cloud radiative properties, *J. Atmos. Sci.*, *56*, 4100–4117, 2000.

Flossmann, A. I., Interaction of aerosol particles and clouds, *J. Atmos. Sci.*, *55*, 879–887, 1998.

Fonner, D., and E. Ganor, The chemical and mineralogical composition of some urban atmospheric aerosols in Israel, *Atmos. Environ., Part B*, *26*, 125–133, 1992.

Früh, B., T. Trautmann, M. Wendisch, and A. Keil, Comparison of observed and simulated NO2 photodissociation frequencies in a cloudless atmosphere and in continental boundary layer clouds, *J. Geophys. Res.*, *105*, 9843–9857, 2000.

Hallett, J., and S. C. Mossop, Production of secondary ice crystals during the riming process, *Nature*, *249*, 26–28, 1974.

Hansen, J., M. Sato, R. Ruedy, I. Tegen, and E. Matthews, Climate forcings in the industrial era, *Proc. Natl. Acad. Sci.*, *95*, 12,753–12,758, 1998.

Harrington, J. Y., T. Reisin, W. R. Cotton, and S. M. Kreidenweis, Cloud resolving simulations of Arctic stratus, II, Transition-season clouds, *Atmos. Res.*, *51*, 45–75, 1999.

Hatzianastassiou, N., W. Wobrock, and A. I. Flossmann, The effect of cloud-processing of aerosol particles on clouds and radiation, *Tellus*, *50*, 478–490, 1998.

Jaenicke, R., Aerosol physics and chemistry, in *Ladolt-Boernstein: Zahlenwerte und Funktionen aus Naturwissenschaften und Technik*, vol. 4b, edited by G. Fischer, pp. 391–457, Springer-Verlag, New York, 1988.

Jiang, H., W. R. Cotton, J. O. Pinto, J. A. Curry, and M. J. Weissbluth, Cloud resolving simulations of mixed-phase Arctic stratus observed during BASE: Sensitivity to concentration of ice crystals and large-scale heat and moisture advection, *J. Atmos. Sci.*, *57*, 2105–2117, 2000.

Krauss, T. W., R. T. Bruintjes, J. Verlinde, and A. Kahn, Microphysical and radar observations of seeded and unseeded continental cumulus clouds, *J. Clim. Appl. Meteorol.*, *26*, 585–606, 1987.

Levin, Z., J. H. Joseph, and Y. Mekler, Properties of Sharav (Khamisin) dust-Comparison of optical and direct sampling data, *J. Atmos. Sci.*, *37*, 882–891, 1980.

Levin, Z., E. Ganor, and V. Gladstein, The effects of desert particles coated with sulfate on rain formation in the eastern Mediterranean, *J. Appl. Meteorol.*, *35*, 1511–1523, 1996.

Meyers, M. P., P. J. DeMott, and W. R. Cotton, New primary ice-nucleation parameterizations in an explicit cloud model, *J. Appl. Meteorol.*, *31*, 708–721, 1992.

Prospero, J. M., Long range transport of mineral dust in the global atmosphere: Impact of African dust on the environment of the southeastern United States, *Proc. Nat. Acad. Sci.*, *96*, 3396–3403, 1999.

Pruppacher, H. R., and J. D. Klett, *Microphysics of Clouds and Precipitation*, 954 pp., D. Reidel, Norwell, Mass., 1997.

Reisin, T. G., Z. Levin, and S. Tzivion, Rain production in convective clouds as simulated in an axissymmetric model with detailed microphysics, II, Effects of varying drop and ice initialization, *J. Atmos. Sci.*, *53*, 1815–1837, 1996.

Rosenfeld, D., Y. Rudich, and R. Lahav, Desert dust suppressing precipitation: A possible desertification feedback loop, *Proc. Nat. Acad. Sci.*, *98*, 5975–5980, 2001.

Twomey, S., The influence of pollution on shortwave albedo of clouds, *J. Atmos. Sci.*, *34*, 1149–1152, 1977.

Tzivion, S., G. Feingold, and Z. Levin, A efficient numerical solution to the stochastic collection equation, *J. Atmos. Sci.*, *44*, 3139–3149, 1987.

Tzivion, S., T. Reisin, and Z. Levin, Numerical simulations of hygroscopic seeding in a convective cloud, *J. Appl. Meteorol.*, *33*, 252–267, 1994.

Wurzler, S., T. G. Reisin, and Z. Levin, Modification of mineral dust particles by cloud processing and subsequent effects on drop size distributions, *J. Geophys. Res.*, *105*, 4501–4512, 2000.

Yin, Y., Z. Levin, T. G. Reisin, and S. Tzivion, The effects of giant cloud condensation nuclei on the development of precipitation in convective clouds-A numerical study, *Atmos. Res.*, *53*, 91–116, 2000a.

Yin, Y., Z. Levin, T. G. Reisin, and S. Tzivion, Seeding convective clouds with hygroscopic flares: Numerical simulations using a cloud model with detailed microphysics, *J. Appl. Meteorol.*, *39*, 1460–1472, 2000b.

Z. Levin, Department of Geophysics and Planetary Sciences, Tel Aviv University, Ramat Aviv 69978, Israel. (zev@hail.tau.ac.il)

T. G. Reisin, Applied Physics Division, Soreq Nuclear Research, Center, Yavne 81800, Israel. (treisin@ndc.soreq.gov.il)

S. Wurzler, Institute for Tropospheric Research, Permoserstrasse 15, D-04303 Leipzig, Germany. (wurzler@tropos.de)

Y. Yin, School of the Environment, University of Leeds, LS2 9JT, UK. (yan@env.leeds.ac.uk)